

## Structure of Ammonium Hydrogen Succinate Above and Below the Phase Transition Around 170 K

A. HIRANO, Y. KUBOZONO, H. MAEDA, H. ISHIDA AND S. KASHINO\*

Department of Chemistry, Faculty of Science, Okayama University, Tsushima, Okayama 700, Japan. E-mail: kashinos@cc.okayama-u.ac.jp

(Received 29 June 1995; accepted 5 September 1995)

### Abstract

For crystals of ammonium hydrogen succinate it is known that the space group is  $P\bar{1}$  with  $Z = 2$  at 293 K and the second-order phase transition occurs around 170 K. X-ray crystal structure analyses above and below 170 K have been carried out in order to study the change in mode of short hydrogen bonds between the hydrogen succinate ions. The space group was determined to be  $P\bar{1}$  at 150 and 190 K by structure analysis. No ordering of the H-atom positions in the short hydrogen bonds occurs by the phase transition. The hydrogen bonds show a decrease in the O...O distances with a decrease in temperature from 290 to 190 K, but no significant change in the geometries between 190 and 150 K. Disorder of the  $\text{NH}_4^+$  ion is not observed at 297, 190 and 150 K. Significant change through the phase transition is found only in the geometry of one of the N—H...O hydrogen bonds between ammonium and hydrogen succinate ions.

### 1. Introduction

The acidic salts of succinic acid ( $\text{MHC}_4\text{H}_4\text{O}_4$ ;  $M = \text{Li}^+$ ,  $\text{Na}^+$ ,  $\text{K}^+$ ,  $\text{Rb}^+$ ,  $\text{Cs}^+$ ,  $\text{NH}_4^+$ ,  $\text{CH}_3\text{NH}_3^+$  and  $\text{C}_2\text{H}_5\text{NH}_3^+$ ) are of much interest, because they have very short hydrogen bonds with O...O 2.41–2.50 Å (McAdam, Currie & Speakman, 1971; McAdam & Speakman, 1971; Küppers, 1982; Kalsbeek, 1991, 1992; Kalsbeek & Larsen, 1991; Haussühl & Schreuer, 1993). The hydrogen succinate ion ( $\text{C}_4\text{H}_5\text{O}_4^-$ ) has no symmetry in the crystals of  $\text{NH}_4^+\cdot\text{C}_4\text{H}_5\text{O}_4^-$  (Haussühl & Schreuer, 1993) and  $\text{C}_2\text{H}_5\text{NH}_3^+\cdot\text{C}_4\text{H}_5\text{O}_4^-$  (Kalsbeek, 1991), but symmetry  $\bar{1}$ , 2 or  $2/m$  in the other acidic salts (McAdam, Currie & Speakman, 1971; McAdam & Speakman, 1971; Küppers, 1982; Kalsbeek & Larsen, 1991; Kalsbeek, 1992).

The second-order phase transition around 170 K has been observed for  $\text{NH}_4^+\cdot\text{C}_4\text{H}_5\text{O}_4^-$  by differential scanning calorimetry (DSC) and thermal expansion measurements (Haussühl & Schreuer, 1993). The crystals of  $\text{NH}_4^+\cdot\text{C}_4\text{H}_5\text{O}_4^-$  are triclinic,  $P\bar{1}$  and  $Z = 2$  at 293 K (Haussühl & Schreuer, 1993). The hydrogen positions in two short hydrogen bonds are equally populated at both sides of each center of symmetry at 293 K and the structure is statistically centrosymmetric (Haussühl

& Schreuer, 1993). A change in space group to  $P1$ , accompanied by an ordering of the hydrogen positions, was expected at lower temperatures than the phase transition temperature,  $T_c$  (Haussühl & Schreuer, 1993). However, this change has not yet been confirmed and no X-ray structure analysis has been carried out below  $T_c$ .

In the present study, the crystal structure analyses of  $\text{NH}_4^+\cdot\text{C}_4\text{H}_5\text{O}_4^-$  have been performed above and below  $T_c$ , in order to ascertain whether the ordering of the hydrogen positions occurs below  $T_c$  and to find any structural change accompanied by the phase transition.

### 2. Experimental

$(\text{NH}_4)_2\text{C}_4\text{H}_4\text{O}_4$  was prepared by adding dry ammonia gas to an ether solution of succinic acid. The white powder obtained was dissolved in water at 313–333 K. Crystals of  $\text{NH}_4^+\cdot\text{C}_4\text{H}_5\text{O}_4^-$  were grown as colorless prisms from the water phase by adding ether and then by slow cooling.

Crystal data and experimental details for structure analyses are collected in Table 1. An X-ray diffraction measurement at 297 K was performed to check the quality of the crystals and the effect of a sapphire stick on reflections. A crystal was mounted on a sapphire stick. The X-ray diffraction data were measured using a Rigaku AFC-5R diffractometer with graphite monochromated  $\text{Mo } K\alpha$  radiation ( $\lambda = 0.71073$  Å) from a 18 kW rotating anode. The intensities were collected using the  $\omega$ - $2\theta$  scan method. The intensities were corrected for Lorentz and polarization effects, but an absorption correction was not applied [ $\mu(\text{Mo } K\alpha) = 0.122$  mm<sup>-1</sup> at 297 K]. Based on the structure reported by Haussühl & Schreuer (1993), non-H atoms were refined anisotropically and H atoms isotropically by a full-matrix least-squares method.  $\sum w(|F_o| - |F_c|)^2$  was minimized with  $w = 1/\sigma^2(F_o)$ . Seven reflections were removed, because they suffered from scattering from the sapphire stick. Correction for the secondary extinction effect was made by  $I_{\text{corr}} = I_o(1 + gI_c)$ , where  $g = 1.13 \times 10^{-5}$ .

Low-temperature diffraction experiments were carried out using an Hüber off-center four-circle diffractometer with graphite-monochromated  $\text{Mo } K\alpha$  radiation. A thermocouple was fixed on a sapphire stick adjacent

Table 1. *Experimental details*

	297 K	190 K	150 K
<b>Crystal data</b>			
Chemical formula	C <sub>4</sub> H <sub>9</sub> NO <sub>4</sub>	C <sub>4</sub> H <sub>9</sub> NO <sub>4</sub>	C <sub>4</sub> H <sub>9</sub> NO <sub>4</sub>
Chemical formula weight	135.119	135.119	135.119
Cell setting	Triclinic	Triclinic	Triclinic
Space group	<i>P</i> $\bar{1}$	<i>P</i> $\bar{1}$	<i>P</i> $\bar{1}$
<i>a</i> (Å)	7.483 (4)	7.437 (1)	7.4384 (6)
<i>b</i> (Å)	8.881 (4)	8.834 (2)	8.8222 (7)
<i>c</i> (Å)	4.731 (4)	4.6927 (6)	4.6875 (6)
$\alpha$ (°)	91.29 (6)	91.32 (1)	91.48 (1)
$\beta$ (°)	93.23 (6)	93.37 (1)	93.178 (9)
$\gamma$ (°)	100.24 (4)	100.68 (1)	100.850 (6)
<i>V</i> (Å <sup>3</sup> )	308.7 (3)	302.25 (8)	301.44 (5)
<i>Z</i>	2	2	2
<i>D<sub>x</sub></i> (Mg m <sup>-3</sup> )	1.453	1.485	1.488
Radiation type	Mo <i>K</i> α	Mo <i>K</i> α	Mo <i>K</i> α
Wavelength (Å)	0.71073	0.71073	0.71073
No. of reflections for cell parameters	25	25	25
$\theta$ range (°)	10–11.5	10–11.5	10–11.5
$\mu$ (mm <sup>-1</sup> )	0.122	0.125	0.125
Temperature (K)	297	190	150
Crystal form	Prism	Prism	Prism
Crystal size (mm)	0.40 × 0.28 × 0.23	0.43 × 0.24 × 0.23	0.43 × 0.24 × 0.23
Crystal color	Colorless	Colorless	Colorless
<b>Data collection</b>			
Diffractometer	Rigaku AFC-5R	Hübler off-center	Hübler off-center
Data collection method	$\omega$ -2 $\theta$	$\omega$ -2 $\theta$	$\omega$ -2 $\theta$
Absorption correction	None	None	None
No. of measured reflections	1593	2416	2406
No. of independent reflections	1285	2184	2175
No. of observed reflections	981	1434	1522
Criterion for observed reflections	$I_o > 3.0\sigma(I)$	$I_o > 3.0\sigma(I)$	$I_o > 3.0\sigma(I)$
Fluctuation of standard reflections	1	2	2
<i>R</i> <sub>int</sub>	0.042	0.067	0.037
$\theta_{\max}$ (°)	27.55	32.0	32.5
Range of <i>h</i> , <i>k</i> , <i>l</i>	-9 → <i>h</i> → 9 -11 → <i>k</i> → 11 0 → <i>l</i> → 6	-11 → <i>h</i> → 11 -13 → <i>k</i> → 13 0 → <i>l</i> → 6	-11 → <i>h</i> → 11 -13 → <i>k</i> → 13 0 → <i>l</i> → 7
No. of standard reflections	3	3	3
Frequency of standard reflections	Every 97 reflections	Every 97 reflections	Every 97 reflections
Intensity decay (%)	1	2	2
<b>Refinement</b>			
Refinement on	<i>F</i>	<i>F</i>	<i>F</i>
<i>R</i>	0.034	0.043	0.038
<i>wR</i>	0.029	0.048	0.043
<i>S</i>	1.49	1.33	1.25
No. of reflections used in refinement	981	1434	1522
No. of parameters used	123	123	123
H-atom treatment	All H-atom parameters refined	All H-atom parameters refined	All H-atom parameters refined
Weighting scheme	$w = 1/\sigma^2(F_o)$	$w = 1/\sigma^2(F_o)$	$w = 1/\sigma^2(F_o)$
( $\Delta/\sigma$ ) <sub>max</sub>	0.41	0.49	0.49
$\Delta\rho_{\max}$ (e Å <sup>-3</sup> )	0.2	0.4	0.3
$\Delta\rho_{\min}$ (e Å <sup>-3</sup> )	-0.2	-0.4	-0.3
Extinction method	$I_{\text{corr}} = I_o(1 + gI_c)$	$I_{\text{corr}} = I_o(1 + gI_c)$	$I_{\text{corr}} = I_o(1 + gI_c)$
Extinction coefficient	$g = 1.13 \times 10^{-5}$	$g = 5.37 \times 10^{-6}$	$g = 4.63 \times 10^{-6}$
Source of atomic scattering factors	Cromer & Waber (1974) for non-H atoms and Stewart, Davidson & Simpson (1992) for H atoms	Cromer & Waber (1974) for non-H atoms and Stewart, Davidson & Simpson (1992) for H atoms	Cromer & Waber (1974) for non-H atoms and Stewart, Davidson & Simpson (1992) for H atoms

to the crystal. The temperatures were regulated within  $\pm 0.7$  K of the setting temperatures using a closed-cycle He refrigerator (Cryogenics, HC-2) equipped with a temperature controller (Cino, KP1000). The cell constants were determined over the temperature range 120–297 K from 25 reflections in the range  $20 < 2\theta < 23^\circ$ . The intensity data at 190 and 150 K were collected by the  $\omega$ -2 $\theta$  scan method and analyzed in the same manner as at 297 K. Three reflections suffering scattering from

the sapphire stick were removed from the data at 190 and 150 K. Correction for a secondary extinction effect was made, where  $g = 5.37 \times 10^{-6}$  at 190 K and  $4.63 \times 10^{-6}$  at 150 K. The structure analyses were performed assuming *P* $\bar{1}$  and *P*1, in order to ascertain the location of H atoms associated with the O—H···O hydrogen bonds. Finally, H-atom peaks were examined by difference-Fourier syntheses on the structures refined by assuming *P* $\bar{1}$  and *P*1.

Atomic scattering factors of non-H atoms were taken from Cromer & Waber (1974) and H atoms from Stewart, Davidson & Simpson (1992). Measurements of X-ray diffraction data were carried out at the X-ray Laboratory of Okayama University. Calculations were performed using the *TEXSAN* crystallographic software package (Molecular Structure Corporation, 1985). Analysis of thermal motion was made using *RSMV-4* (Ito & Sakurai, 1967).

Differential thermal analysis (DTA) and differential scanning calorimetry (DSC) were carried out using a home-made apparatus (Kume, Ikeda & Nakamura, 1979) and a Perkin-Elmer DSC-7, respectively.

### 3. Results and discussion

The temperature dependence of cell constants is shown in Fig. 1. The atomic parameters are listed in Table 2.\* The thermal ellipsoids of  $\text{NH}_4^+ \cdot \text{C}_4\text{H}_5\text{O}_4^-$  with atomic numbering are illustrated in Fig. 2. Molecular geometries are listed in Table 3. The crystal structure at 150 K is illustrated in Fig. 3. Geometries of hydrogen bonds are listed in Table 4.

The dimension of *a* decreases with a decrease in temperature in the range above 170 K, but increases below 170 K. The dimensions of *b* and *c* decrease with a decrease in temperature over all ranges, but show a slight bending around  $T_c$ . The effect of the phase transition is also reflected in  $\alpha$ ,  $\beta$ ,  $\gamma$  and *V*. From the temperature dependence of cell constants,  $T_c$  has been determined to be 170 K, which is comparable with that reported at 169 K (Haussühl & Schreuer, 1993).

The change in cell constants is reversible for cooling and heating through  $T_c$ . In order to confirm the phase transition and to determine  $T_c$ , DTA curves were recorded in the temperature range 100–300 K. When the sample was heated and cooled, a small heat anomaly accompanying a long tail on the low-temperature side was observed at the same peak temperature of 170 (1) K. The enthalpy change at the transition determined by DSC was  $27 \text{ J mol}^{-1}$ , in agreement with that reported previously,  $32 \text{ J mol}^{-1}$  (Haussühl & Schreuer, 1993). Consequently, it has been concluded that  $\text{NH}_4^+ \cdot \text{C}_4\text{H}_5\text{O}_4^-$  shows the phase transition around 170 K.

As shown in Fig. 4, each peak around (0, 0, 0) and  $(\frac{1}{2}, \frac{1}{2}, 0)$  in difference-Fourier maps at 150 K is split into both sides of the middle point between two O atoms, not only in the  $P\bar{1}$  structure but also in *P1*. At 190 K the peak splitting is observed in the  $P\bar{1}$  and *P1* structures, as found at 150 K. From these facts it is concluded that the space group is  $P\bar{1}$  at 150, 297 and 190 K. Thus, an ordering of the H-atom positions does not contribute to

the phase transition in the present system. However, it is noted that there is a report suggesting an ordering of the H atoms by a second-order phase transition for the system  $\text{CaHPO}_4$  (Catti & Ferraris, 1980).

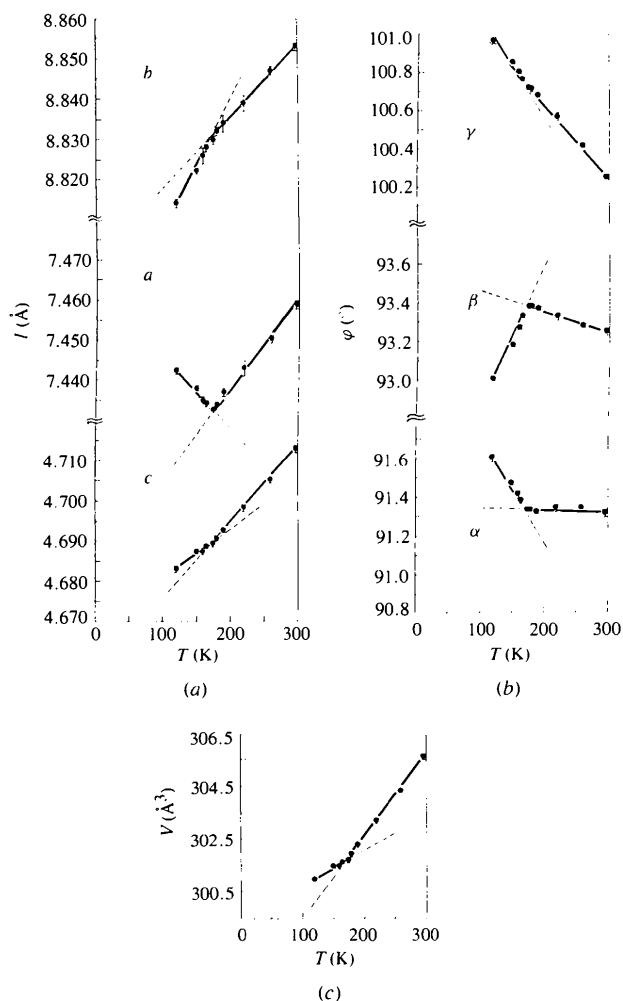


Fig. 1. The lattice constants as a function of temperature. (a) *a*, *b*, *c* versus *T*, (b)  $\alpha$ ,  $\beta$ ,  $\gamma$  versus *T* and (c) *V* versus *T*.

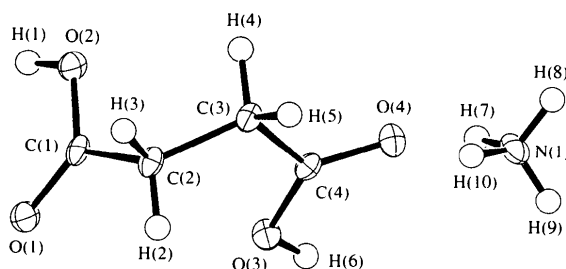


Fig. 2. The displacement ellipsoids (50% probability) at 150 K with atomic numbering for the  $P\bar{1}$  structure. The H atoms are represented as spheres equivalent to  $B = 1.0 \text{ \AA}^2$ .

\* Lists of atomic coordinates, anisotropic displacement parameters and structure factors have been deposited with the IUCr (Reference: AS0697). Copies may be obtained through The Managing Editor, International Union of Crystallography, 5 Abbey Square, Chester CH1 2HU, England.

Table 2. Fractional atomic coordinates and equivalent isotropic displacement parameters ( $\text{\AA}^2$ ) for  $P\bar{1}$ 

$$B_{\text{eq}} = (8\pi^2/3)\sum_i \sum_j U_{ij} a_i^* a_j^* \mathbf{a}_i \cdot \mathbf{a}_j.$$

	<i>x</i>	<i>y</i>	<i>z</i>	<i>B</i> <sub>eq</sub>
190 K				
O(1)	0.3038 (2)	0.0318 (1)	0.2482 (3)	1.93 (4)
O(2)	0.0325 (1)	0.1007 (1)	0.1940 (2)	1.57 (4)
O(3)	0.4131 (2)	0.4162 (1)	0.1693 (2)	1.61 (4)
O(4)	0.2729 (2)	0.6129 (1)	0.2532 (2)	1.75 (4)
N(1)	0.3271 (2)	0.8082 (2)	-0.2277 (4)	1.87 (5)
C(1)	0.1940 (2)	0.1124 (2)	0.3177 (3)	1.32 (5)
C(2)	0.2392 (2)	0.2292 (2)	0.5634 (3)	1.40 (5)
C(3)	0.1846 (2)	0.3833 (2)	0.5051 (3)	1.42 (5)
C(4)	0.2969 (2)	0.4800 (2)	0.2958 (3)	1.22 (4)
150 K				
O(1)	0.3036 (1)	0.0315 (1)	0.2486 (2)	1.67 (3)
O(2)	0.0326 (1)	0.1008 (1)	0.1957 (2)	1.32 (3)
O(3)	0.4132 (1)	0.4162 (1)	0.1702 (2)	1.37 (3)
O(4)	0.2734 (1)	0.6133 (1)	0.2546 (2)	1.44 (3)
N(1)	0.3274 (2)	0.8086 (1)	-0.2264 (3)	1.59 (4)
C(1)	0.1939 (2)	0.1125 (1)	0.3192 (3)	1.18 (4)
C(2)	0.2392 (2)	0.2291 (1)	0.5658 (3)	1.17 (4)
C(3)	0.1851 (2)	0.3836 (1)	0.5086 (3)	1.16 (4)
C(4)	0.2974 (2)	0.4802 (1)	0.2977 (3)	1.05 (4)

Table 3. Bond lengths ( $\text{\AA}$ ) and angles ( $^\circ$ ) of  $\text{NH}_4^+ \cdot \text{C}_4\text{H}_5\text{O}_4^-$ 

	297 K	190 K	150 K
C(1)—C(2)	1.507 (2)	1.509 (1)	1.508 (1)
C(2)—C(3)	1.519 (3)	1.517 (1)	1.518 (1)
C(3)—C(4)	1.506 (2)	1.504 (1)	1.506 (1)
C(1)—O(1)	1.233 (1)	1.231 (1)	1.234 (1)
C(1)—O(2)	1.290 (1)	1.288 (1)	1.288 (1)
C(4)—O(3)	1.281 (1)	1.282 (1)	1.281 (1)
C(4)—O(4)	1.240 (1)	1.239 (1)	1.240 (1)
O(1)—C(1)—O(2)	123.1 (1)	123.1 (1)	123.0 (1)
O(1)—C(1)—C(2)	121.5 (2)	121.5 (1)	121.5 (1)
O(2)—C(1)—C(2)	115.3 (2)	115.4 (1)	115.4 (1)
O(3)—C(4)—O(4)	123.9 (2)	124.0 (1)	123.9 (1)
O(3)—C(4)—C(3)	116.2 (2)	116.2 (1)	116.2 (1)
O(4)—C(4)—C(3)	119.9 (1)	119.8 (1)	119.8 (1)
C(1)—C(2)—C(3)	115.0 (2)	114.5 (1)	114.4 (1)
C(2)—C(3)—C(4)	115.7 (1)	115.2 (1)	115.1 (1)

In the crystal of  $\text{NH}_4^+ \cdot \text{C}_4\text{H}_5\text{O}_4^-$ , two short  $\text{O}—\text{H} \cdots \text{O}$  hydrogen bonds are formed between  $\text{C}_4\text{H}_5\text{O}_4^-$  ions related by  $\bar{1}$  at  $(0, 0, 0)$  and  $(\frac{1}{2}, \frac{1}{2}, 0)$ . At all temperatures, H(1) and H(6) atoms in the short hydrogen bonds are equally populated on both sides. The  $\text{O}—\text{H} \cdots \text{O}$  hydrogen bond distances decrease with a decrease in temperature from 297 to 190 K, as seen from Table 4, while there are no significant changes in the distances between 190 and 150 K.

Difference-Fourier maps calculated by removing the four H atoms of the  $\text{NH}_4^+$  ion at 297, 190 and 150 K showed neither disorder of the H atoms nor peak broadening. The  $\text{NH}_4^+$  ion participates in five  $\text{N}—\text{H} \cdots \text{O}$  hydrogen bonds, as seen from Table 4. The H(8) atom of the  $\text{NH}_4^+$  ion is involved in a bifurcated hydrogen bond.

Table 4. Geometries ( $\text{\AA}, ^\circ$ ) of hydrogen bonds

	<i>D</i> ... <i>A</i>	<i>D</i> — <i>H</i>	<i>H</i> ... <i>A</i>	<i>D</i> — <i>H</i> ... <i>A</i>
O(2)—H(1)···O(2 <sup>i</sup> )				
297 K	2.502 (2)	0.86 (4)	1.64 (4)	179 (4)
190 K	2.478 (2)	0.93 (6)	1.58 (6)	162 (6)
150 K	2.485 (2)	0.86 (4)	1.62 (4)	178 (4)
O(3)—H(6)···O(3 <sup>ii</sup> )				
297 K	2.479 (2)	0.84 (5)	1.65 (5)	177 (5)
190 K	2.455 (2)	0.87 (5)	1.60 (5)	168 (5)
150 K	2.456 (2)	0.86 (5)	1.60 (5)	172 (5)
N(1)—H(9)···O(1 <sup>ii</sup> )				
297 K	2.883 (2)	0.95 (2)	1.95 (2)	169 (2)
190 K	2.853 (2)	0.90 (2)	1.95 (2)	174 (2)
150 K	2.849 (1)	0.87 (2)	1.98 (2)	174 (2)
N(1)—H(10)···O(4)				
297 K	2.894 (2)	0.96 (2)	1.95 (2)	167 (2)
190 K	2.874 (2)	0.95 (2)	1.94 (2)	168 (2)
150 K	2.873 (1)	0.94 (2)	1.95 (2)	167 (2)
N(1)—H(8)···O(2 <sup>iii</sup> )				
297 K	2.956 (2)	0.86 (3)	2.18 (3)	149 (3)
190 K	2.944 (2)	0.85 (2)	2.14 (2)	159 (2)
150 K	2.945 (2)	0.88 (3)	2.14 (3)	152 (3)
N(1)—H(7)···O(4 <sup>iv</sup> )				
297 K	2.963 (2)	0.94 (3)	2.05 (3)	164 (3)
190 K	2.917 (2)	0.96 (3)	1.97 (3)	170 (3)
150 K	2.909 (1)	0.93 (3)	1.99 (3)	169 (3)
N(1)—H(8)···O(1 <sup>v</sup> )				
297 K	2.981 (2)	0.86 (3)	2.47 (3)	119 (2)
190 K	2.981 (2)	0.85 (2)	2.59 (2)	110 (2)
150 K	2.967 (1)	0.88 (3)	2.50 (3)	114 (2)

Symmetry codes: (i)  $-x, -y, -z$ ; (ii)  $1-x, 1-y, -z$ ; (iii)  $-x, 1-y, -z$ ; (iv)  $x, y, z-1$ ; (v)  $x, 1+y, z$ .

The  $\text{N} \cdots \text{O}$  distances except  $\text{N} \cdots \text{O}(1^v)$  decrease with a decrease in temperature from 297 to 190 K. The  $\text{N}—\text{H}(8) \cdots \text{O}(1^v)$  hydrogen bond is weakened by the decrease in temperatures from 297 to 190 K, as seen from the  $\text{H}(8) \cdots \text{O}(1^v)$  distances and the  $\text{N}—\text{H} \cdots \text{O}$  angles. The  $\text{N} \cdots \text{O}(1^v)$  distance at 150 K is significantly

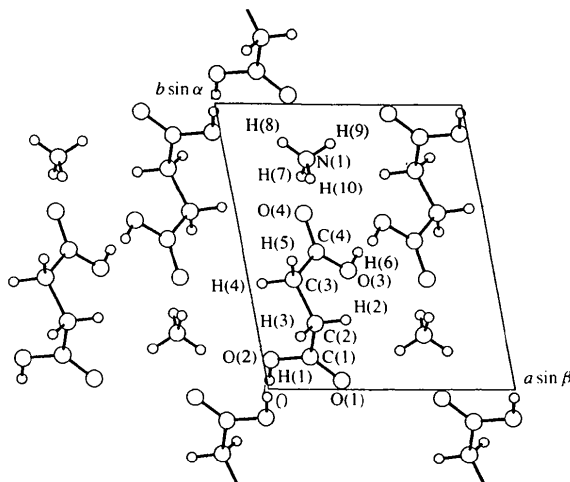


Fig. 3. Projection of the crystal structure of  $\text{NH}_4^+ \cdot \text{C}_4\text{H}_5\text{O}_4^-$  along the *c* axis ( $P\bar{1}$  at 150 K).

Table 5.

(a) Principal axes  $P_i$  of moment of Inertia  $I$ .

$P_i = l \cdot \mathbf{a} + m \cdot \mathbf{b} + n \cdot \mathbf{c}$  ( $i = 1, 2, 3$ ), where  $\mathbf{a}$ ,  $\mathbf{b}$  and  $\mathbf{c}$  refer to the unit vectors along the respective crystallographic axes.  $I = \sum m_i r_i^2$ ;  $m_i$  is a mass and  $r_i$  is the distance to the principle axis from atom  $i$ .  $R_G = (r_i^2)^{1/2}$ ;  $R_G$  is the root-mean-square radius of gyration.

	Axis	$I$ (amu $\text{\AA}^2$ )	$R_G$ ( $\text{\AA}$ )	$l$	$m$	$n$
297 K	$P_1$	103.289	0.961	0.02708	0.11439	-0.00050
	$P_2$	380.419	1.843	-0.11938	0.00392	0.08217
	$P_3$	411.026	1.916	0.05938	0.00276	0.19520
190 K	$P_1$	103.411	0.961	0.02722	0.11517	-0.00058
	$P_2$	377.441	1.836	-0.12006	0.00316	0.08315
	$P_3$	407.957	1.909	0.06038	0.00333	0.19674
150 K	$P_1$	103.662	0.962	0.02723	0.11540	-0.00052
	$P_2$	376.642	1.834	-0.11996	0.00296	0.08421
	$P_3$	406.934	1.906	0.06063	0.00366	0.19652

(b) Most probable values of the molecular vibrational tensors of the  $\text{C}_4\text{H}_5\text{O}_4^-$  ion

	$T$ ( $\text{\AA}^2$ )			$L$ ( $\text{deg}^2$ )		
297 K	0.026 (2)	-0.000 (1)	0.000 (2)	35 (6)	-2 (2)	8 (3)
	0.022 (2)	-0.002 (2)	0.022 (3)	9 (2)	1 (2)	7 (2)
	0.015 (1)	-0.001 (1)	-0.002 (1)	22 (4)	-2 (1)	4 (2)
190 K	0.013 (1)	-0.002 (1)	0.014 (2)	5 (1)	1 (1)	4 (1)
	0.013 (1)	0.001 (1)	-0.001 (1)	14 (3)	-2 (1)	3 (1)
	0.014 (1)	-0.001 (1)	0.012 (1)	3 (1)	0.4 (8)	2.9 (9)

shorter than those at 297 and 190 K. The  $\text{H}(8) \cdots \text{O}(1^v)$  distance and  $\text{N}-\text{H}(8) \cdots \text{O}(1^v)$  angle show that the hydrogen bond is again strengthened below  $T_c$ . The  $\text{N} \cdots \text{O}$  distances of the other  $\text{N}-\text{H} \cdots \text{O}$  hydrogen bond show no significant differences between 190 and 150 K.

In order to find any anomaly in thermal motions, the thermal motions at 297, 190 and 150 K were analyzed.

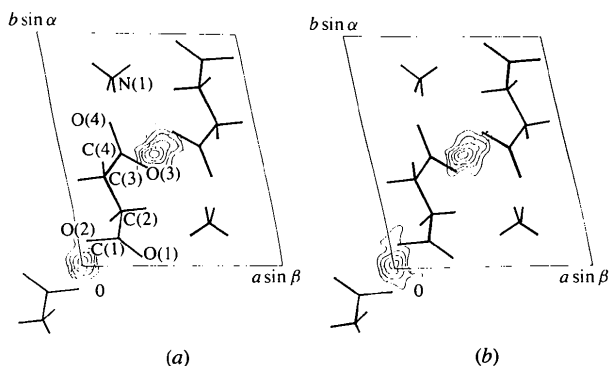


Fig. 4. Difference-Fourier maps viewed down the  $c$  axis, showing two peaks around the centers between O atoms: (a) by assuming  $P_1$  at 150 K and (b) by assuming  $P_1$  at 150 K. Contours are drawn by solid lines for the section where  $Z = 0.05$  and by broken lines for the section where  $Z = -0.05$  with intervals of  $0.1 \text{ e } \text{\AA}^{-3}$ , starting at  $0.1 \text{ e } \text{\AA}^{-3}$ .

The results are summarized in Table 5. The principal axes of the moment of inertia for the  $\text{C}_4\text{H}_5\text{O}_4^-$  ion are used to describe the translational ( $T$ ) and librational ( $L$ ) motions. The components of  $T$  and  $L$  with respect to each principal axis decrease with a decrease in temperature in the same manner. Although a librational motion around a long molecular axis  $P_1$  is remarkably larger than those around  $P_2$  and  $P_3$ , the temperature dependency is almost equal. The conformation of the  $\text{C}_4\text{H}_5\text{O}_4^-$  ion is *gauche*;  $\text{C}(1)-\text{C}(2)-\text{C}(3)-\text{C}(4) = -70.4(2)^\circ$  at 297 K,  $-70.6(2)^\circ$  at 190 K and  $-70.2(1)^\circ$  at 150 K, while the conformation is *trans* in many other acidic salts of alkaline metals (McAdam, Currie & Speakman, 1971; McAdam & Speakman, 1971; Küppers, 1982; Kalsbeek, 1991, 1992; Kalsbeek & Larsen, 1991; Haussühl & Schreuer, 1993). The torsion angle and r.m.s. radius of gyration around each principal axis show no remarkable difference in molecular conformations for all temperatures.

The authors wish to express their thanks to Professor Yoshio Nogami of Okayama University for his valuable discussion and to Professor Siegfried G. Haussühl of Köln University for his valuable suggestions for sample preparation.

## References

- Catti, M. & Ferraris, G. (1980). *Acta Cryst.* B36, 254–259.
- Cromer, D. T. & Waber, J. T. (1974). *International Tables for X-ray Crystallography*, Vol. IV, Table 2.2A, pp. 149–150. Birmingham: Kynoch Press. (Present distributor Kluwer Academic Publishers, Dordrecht.)
- Haussühl, S. G. & Schreuer, J. (1993). *Z. Kristallogr.* 206, 255–265.
- Ito, T. & Sakurai, T. (1967). *RSMV-4. The Universal Crystallographic Computing System (I)*, pp. 83–84. The Crystallographic Society of Japan, Tokyo, Japan.
- Kalsbeek, N. (1991). *Acta Cryst.* C47, 1649–1653.
- Kalsbeek, N. (1992). *Acta Cryst.* C48, 1389–1394.
- Kalsbeek, N. & Larsen, S. (1991). *Acta Cryst.* C47, 1005–1009.
- Kume, Y., Ikeda, R. & Nakamura, D. (1979). *J. Magn. Reson.* 33, 331–344.
- Küppers, H. (1982). *Z. Kristallogr.* 159, 85–86.
- McAdam, A. & Speakman, J. C. (1971). *J. Chem. Soc. A*, pp. 1997–1999.
- McAdam, A., Currie, M. & Speakman, J. C. (1971). *J. Chem. Soc. A*, pp. 1994–1997.
- Molecular Structure Corporation (1985). *TEXSAN. TEXRAY Structure Analysis Package*. MSC, 3200 Research Forest Drive, The Woodlands, TX 77381, USA.
- Stewart, R. F., Davidson, E. R. & Simpson, W. T. (1992). *International Tables for X-ray Crystallography*, Vol. C, p. 487. Dordrecht: Kluwer Academic Publishers.